Light & Engineering
Vol. 28, No. 3, pp. 87–97, 2020

https://doi.org/10.33383/2019–048
Svetotekhnika #1, 2020, pp. 76–84

DESIGN, DEVELOPMENT AND PRACTICAL REALIZATION OF A VLC SUPPORTIVE INDOOR LIGHTING SYSTEM

Sourish Chatterjee and Biswanath Roy*

Illumination Engineering Laboratory, Electrical Engineering Department,
Jadavpur University, Kolkata, India
**E-mail: broy@ee.jdvu.ac.in*

ABSTRACT

In an office space, an LED-based lighting system allows you to perform the function of a data transmitter. This article discusses the cost-effective design and development of a data-enabled LED driver that can transmit data along with its receiving part. In addition, this paper clearly outlines the application of the proposed VLC system in an office environment where ambient light interference is a severe issue of concern. The result shows satisfactory lighting characteristics in general for this area in terms of average horizontal illuminance and illuminance uniformity. At the same time, to evaluate real-time and static communication performance, *Arduino* interfaced *MATLAB Simulink* model is developed, which shows good communication performance in terms of BER (10^{-7}) even in presence of ambient light noise with 6 dB signal to interference plus noise ratio. Our designed system is also flexible to work as a standalone lighting system, whenever data communication is not required.

Keywords: data-enabled LED driver, visual light communication (VLC), optical receiver, bit error rate (BER), ambient light interference

1. INTRODUCTION

In recent years of energy crisis, light emitting diodes (LEDs) evolves as a major alternative in the field of lighting technology due to their higher efficacy and longer life [1, 2, 3]. This lighting revolution has changed the application of conventional electric lamps, especially in the indoor. At the same time, increasing the switching speed of this solid-state device creates a unique opportunity for high-speed data transmission [4]. With the advent of LEDs, visible light communication (VLC) emerged as potential alternatives to radio frequency solutions [5, 6]. Moreover, there are some notable advantages of VLC systems over radio frequency and infrared frequency-based systems, which are:

– So far there is no regulation regarding the use of visible electromagnetic spectrum;

– Unlike the infrared communication schemes, there is no health regulation to restrict the transmit power; so, adaptation of this type of communication will be highly accepted at hospitals and health centres [7].

It is known that the switching frequency of white LED is slower than its coloured counterpart, though it can support data rate in Mbps [8, 9]. It has already been reported that visible light wireless point-to-point communication link at 513 megabit per second [10]. In some other work, it was shown that smaller area micro-LED pixels generally exhibit higher modulation bandwidth than their larger area counterparts [11]. In this context, white LED evolves as a potential illuminant for high-speed short-range line of sight data transmitter. The primary objective of using white LED in lighting applications is to provide energy-efficient lighting solutions. In earlier works, researchers worked on different techniques to transmit the data through visible spectrum [12]. However, there has been little research on the practical implementation of the

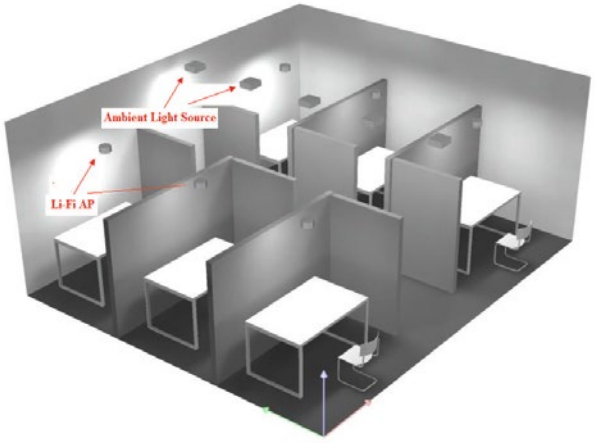

Fig. 1. 3-D view of Li-Fi supportive LED lighting system at office cubicle

VLC system to achieve substantial communication performances in presence of ambient daylight and other artificial light sources [13, 14]. Din and Kim achieved both the objectives of VLC through computer simulation [15], but they did not consider the practical realization of their system and the effect of ambient light at the time of data transmission. In the reference [16], average illuminance less than 50 lx was achieved at the distance of 80 cm from transmitter to receiver. Usually, in case of indoor lighting available daylight can be integrated with the artificial source to save energy. Therefore, data transmission through VLC in presence of diffused daylight and/or other artificial light sources is another area of concern. In the reference [14], a new optical receiver is proposed to reduce ambient light noise. Data communication was established by the proposed system at a data rate of 10 kbps from 0.4 m distance. However, the applicability of this system was not demonstrated inside an indoor environment. Moreover, bit error rate (BER) of their proposed system had not been evaluated either.

In contrast to the earlier work, we have demonstrated a practical solution for installing a VLC system in an office area. The proposed VLC system is also flexible to use as a normal light source whenever data transmission is not required. The communication performance of our proposed system is evaluated in presence of daylight and ambient light sources (ALS). The result shows better communication performance from 1 m distance in presence of ambient light interferences. In addition, the lighting requirements across all the working areas inside the office space are accomplished in terms of average horizontal illuminance and illuminance uniformity.

The rest of the paper is organized as follows. Section 2 is devoted to the room geometry and its stages of implementation. In section 3, system model is discussed. The design of transmitter and receiver sections are demonstrated in section 4 and 5 respectively. Sections 6 and 7 provide guidance on evaluating the effectiveness of lighting and communication. Finally, all results are compiled in section 8 for subsequent discussion and analysis.

2. ROOM GEOMETRY AND EXECUTION STEPS

The office room with dimension (7×6×3) m is subdivided into six parts of small cubicles, as shown in Fig. 1. The width of the corridor inside the room is taken as 1.6 m and the dimension of each working area inside a cubicle is the (1.5×0.85) m. For each cubicle, separate access point (AP) with zero co-channel interference (CCI) was selected. The white light emitting diode (WLED) installed at each AP is capable of transmitting the data through intensity modulation. Moreover, it can fulfil the major lighting requirement over the working area. Apart from these WLEDs, compact fluorescent lamps (CFL) are also installed inside the office space to maintain good illuminance uniformity and required horizontal illuminance throughout the scene.

As per the ISO standard [17], for an office environment, the required minimum supported average illuminance on working surface is 300 lx. The main objectives of this work are to provide required

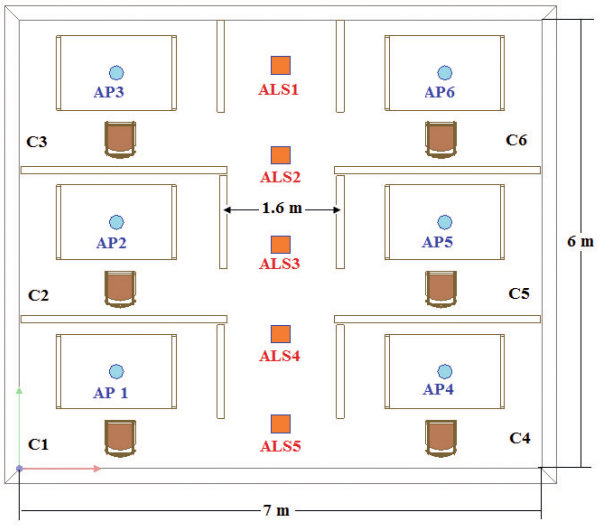

Fig. 2. View from the top of the office space (C – cubicle, ALS – ambient light source, AP – access point)

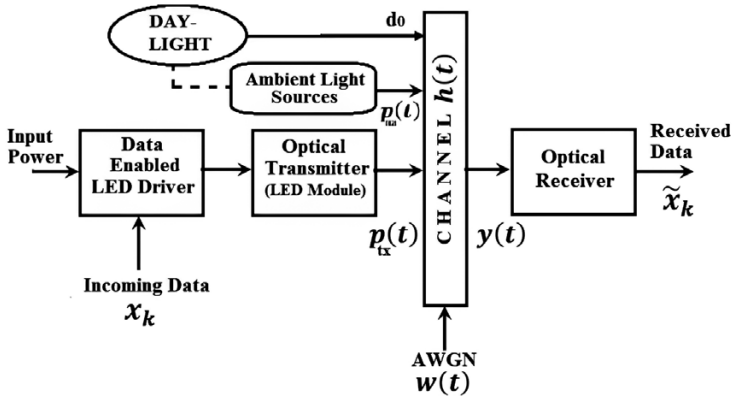

Fig. 3. Block diagram of the proposed VLC system, where AWGN – additive white Gaussian noise

illuminance at the expense of less power and at the same time to use some of the light sources as an AP with higher accuracy in terms of bit error rate. The diffused daylight can be integrated with the ambient light sources to save energy during daytime. Daylight is also a potential source of noise if we consider our system from communication perspective. Therefore, the goal of the project is to implement and evaluate the performance of a prototype system that can transmit data with minimum error even in presence of ambient light noise and provide sufficient illuminance on the working surface.

The desired lighting and communication characteristics of the proposed system are achieved by performing the following steps:

– A low cost LED driver is designed, which is capable of transmitting data as well; the objective to design the integrated data-enabled LED driver is of two-fold: the first one is to drive the LED module at a rated voltage and current so that the required illuminance can be achieved and the second is to act as a data transmitter;

– The optical receiver is designed to receive transmitted data by deflecting noise generated by daylight and other ambient lighting sources;

– A DIALux simulation of the specified office environment, consisting of six cubicles, was done to determine the illumination contribution of ALS on working areas; the view from the top of the office space is shown in Fig. 2, and since the attributes of all six cubicles (C1-C6) are similar and CCI are not considered, it is good enough to test the communication efficiency experimentally for a single unit;

– Initially, the communication performance of a single unit is evaluated using a random bit pattern in presence of ambient daylight, after what *MATLAB Simulink* and *Arduino* interface is used to test the system for a real-time long stream of data in presence of ambient light interferences, whereupon the impact of ambient light noise on bit error rate (BER) and signal to interference plus noise ratio (SINR) are also reported with the help of experimentally obtained results.

3. BLOCK DIAGRAM OF THE OWC SYSTEM

The geometry of an optical wireless communication (OWC) scenario is determined by the position and detection characteristics of the transmitter and receiver in the room. The block diagram of the designed OWC system is illustrated in Fig. 3.

The incoming binary data is optically modulated using the data enabled LED driver briefly discussed in section 4. Furthermore, this LED driver supplied sufficient direct current to the arrays of LED, so that average horizontal illuminance fulfils ISO recommendation. The optically modulated signal is then transmitted over an optical wireless channel before the optical receiver receives it. Ambient luminous flux, introduced by daylight and artificial light source also propagates through the channel and acts as unwanted interference to the optical receiver. The optical channel can be considered as a linear, time-invariant, memory-free system with an impulse response of a finite duration [18]. If there is an ambient light, it can be described by the following continuous time model for a noisy communication line:

$$y(t) = h(t) * \left[p_{tx}(t) + p_{na}(t) \right] + d_0 + w(t), \quad (1)$$

where $p_{tx}\ (t)$ represents the intensity-modulated transmitted signal by the LED source and $y(t)$ denotes received distorted replica of the transmitted signal. The interference due to ambient light sources and received noise due to daylight are denoted by $p_{na}\ (t)$ and d_0 respectively. Although the daylight is

dynamic in nature, the rate of variation is negligible in comparison with p_{tx} *(t)* and p_{na} *(t)*. Therefore, we can assume that the daylight provides a DC offset d_0 to the optical receiver. At the receiving end, the amplitude of the received voltage signal is proportional to the integral of the incident optical power over the area of the photodiode. The shot and thermal noise introduced at the receiver, *w (t),* can be considered as additive white Gaussian noise (AWGN) [19].

The pulse characteristic of the channel, *h (t),* can be approximated by a scalable and lagging Dirac delta function for the line of sight (LOS) link as considered in our system. It is given by [20]

$$h(t) = \frac{(m+1)A_R}{2\pi d^2} \cdot cos^m(\varphi) \cdot cos(\theta) \times \\ \times rect\left(\frac{\theta}{FOV}\right) \cdot \delta \cdot \left(t - \frac{d}{C}\right), \quad (2)$$

where A_R is the receiver area, FOV is the field of view of detector, d is the distance between LED and detector surface, φ is the angle of irradiance, θ is the angle of incidence, c is the velocity of light, and m is the order of Lambert emission which can be determined using the transmitter half-angle (α_H) given by [21, 22] as:

$$\alpha_H = \cos^{-1} 0.5^{1/m}. \quad (3)$$

In case of single path LOS channel the term $\delta\left(t - \frac{d}{C}\right)$ can be dropped and the effect of the channel is fully represented by the channel DC gain $H(0)$ given by

$$H(0) = \int_{-\infty}^{\infty} h(t)dt. \quad (4)$$

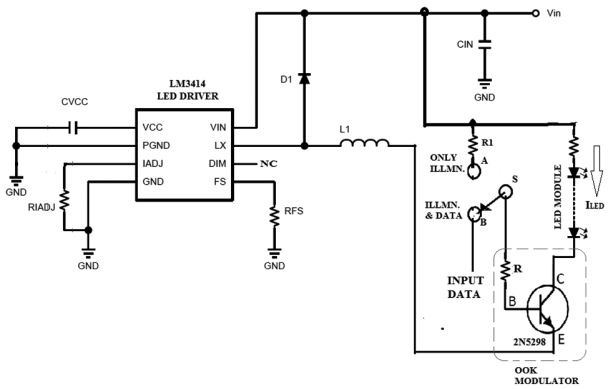

Fig. 4. Integrated data-enabled LED driver using LM3414

Point specific horizontal illuminance (E_0) over the working area in any cubicle is given by

$$E_0 = E_{AP} + E_{AL}, \quad (5)$$

where E_{AP} is the illuminance, contributed by the optical transmitter at access point, E_{AL} is the illuminance contributed by ambient light.

4. DESIGN OF INTEGRATED DATA ENABLED LED DRIVER

An integrated data-enabled LED driver is a special type of LED driver, which is capable of controlling the LED module at rated current and transmitting the data through intensity modulation simultaneously. The circuit diagram of our proposed driver is shown in Fig. 4. Binary amplitude shift keying (BASK) or on-off keying (OOK) is one of the simplest digital modulation techniques, which is used here to transmit digital data using the optical source, i.e. LED matrix. Binary 1 is represented by a short pulse of light and binary 0 by the absence of light.

The data to be transmitted is applied at the INPUT DATA pin of the designed driver, while the switch is connected with point B at the time of data transfer. In order to achieve OOK data transfer method the transistor 2N5298 is used, which acts as a high-speed switching device. As we have mentioned earlier, the user can only use the system for lighting purposes, as well, and at that time switch is connected to position A. In this work, six LEDs with sufficient switching frequency were connected in series to fabricate the optical transmitter. Each LED has forward voltage drop of 2.7 V and capable of handling 700 mA maximum current. The power rating of each LED is 2 W. IC LM3414 used as a 1 A 60 W common anode constant current LED buck driver to drive the LED module at rated current (I_L is taken as 350 mA).

The LM3414 is a PWM LED driver that contains a clock generator to generate constant switching frequency for the device. The switching frequency is determined by the resistance of an external resistor R_{FS} in the range of 250 kHz to 1 MHz. The lower resistance of R_{FS} results in higher switching frequency. The switching frequency of the LM3414/14HV is given by equation [23]

$$f_{sw} = \frac{20 \cdot 10^6}{R_{FS}}. \quad (6)$$

Table 1. Design Parameters of Data Enabled LED Driver

Design Parameters		Value
Description	Symbol	
Input voltage (DC)	V_{IN}	24 V
Forward voltage drop across LED array	V_{LED}	16.2 V
Average LED current	I_{LED}	350 mA
Internal switching frequency	f_{SW}	500 kHz
Switching frequency selective resistor	R_{FS}	40 kΩ
Current control resistor	R_{IADJ}	8.92 kΩ
Minimum value of inductor L_1	L_{MIN}	25.3 µH

To ensure correct regulation of the output current, the LM3414 operates in continuous conduction mode (CCM). With PWM enabled, the peak-to-peak inductor current ripple can be set as high as ± 60 % of the defined average output current. The defined average LED current and allowable inductor current ripple decides the minimum inductance of the inductor. The minimum inductance can be found by the equation

$$L_{MIN} = \frac{V_{IN} - V_{LED}}{1.2 I_{LED}} \cdot \frac{V_{LED}}{V_{IN}} \cdot \frac{1}{f_{SW}}. \quad (7)$$

Using equations (6) and (7), the calculated parameters are summarized in Table 1.

5. DESIGN OF OPTICAL RECEIVER

The block diagram of the proposed optical receiver section is shown in Fig. 5, which comprises of three major units.

The front end of the optical detector is designed using a photodiode (PD) and trans-impedance amplifier (TIA) with 'auto-zero' feedback loop. The second stage comprises of an interference rejection filter (IRF) followed by a Butterworth low pass filter (LPF). The detailed circuit diagram of these first two stages is shown in Fig. 6.

The photodiode converts optical and electrical signals (O/E). The 'auto-zero' feedback loop associated with TIA is developed to maintain 0 V DC output in the absence of transmitted pulse. Any DC error present at output A1 generates the opposite signal at output A2. Subsequently, a correction voltage becomes evident at A1 non-inverting input to bring A1 output back to zero. The lower cut off frequency of the amplifier is set with resistor R5 and capacitor C3, while the upper cut off frequency is set with R3 and C2. The bandwidth of the designed TIA is 800 kHz with a gain of 10. This unit removes any DC offset primarily originated by the ambient daylight. The second stage has been designed with the objective of detecting the weak signal and bypassing the interference due to harmonics of ALS (compact fluorescent lamps are used here).

The major photodiode response due to this interfering signal can be expressed as [24]

$$I_{ALS}(t) = kI_{av} \sum_{i=1}^{20} \begin{bmatrix} m_i \cos\{(2\pi 100i - 50)t + \chi_i \\ + n_i \cos(2\pi 100it + \xi_i)\} \end{bmatrix}, \quad (8)$$

where I_{av} is the average current through the ambient light source, k is the constant of interference proportionality, m_i and n_i are the amplitudes of odd and even harmonics of 50 Hz, χ_i and ξ_i are the phases of odd and even harmonics respectively.

Equation (8) assumes that the interferences due to CFLs dominate within 2000 Hz. To eliminate these interferences caused by ambient light sources, it is proposed to use an interference rejection filter (IRF). The interference rejection filter is a unit gain high pass Bessel filter with cut off frequency of 2 kHz. Followed by the IRF a low pass Butterworth

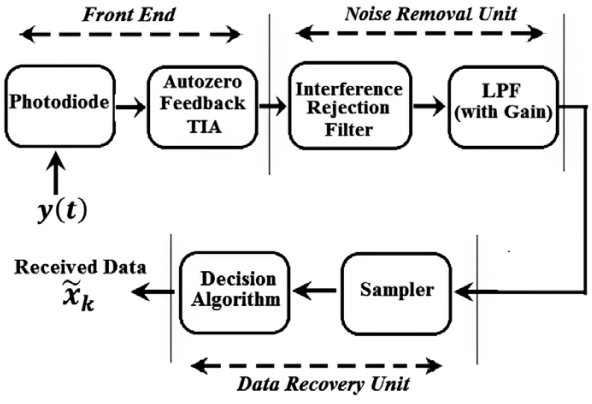

Fig. 5. Block diagram of the proposed optical receiver

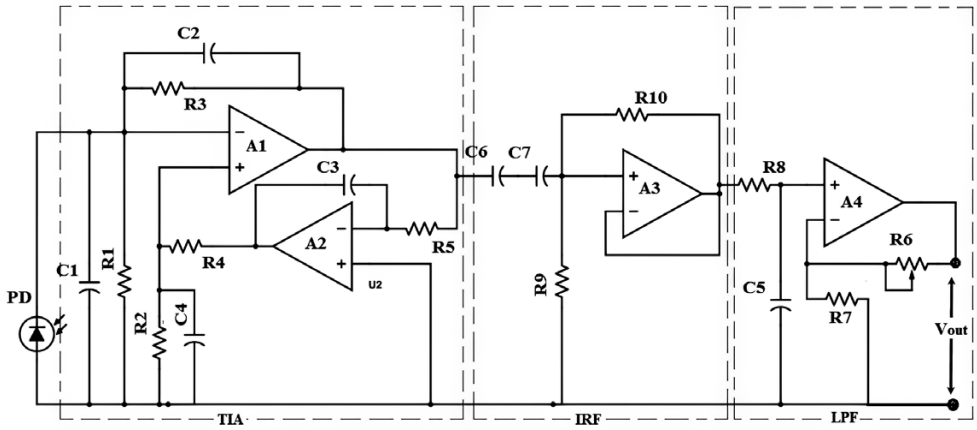

Fig. 6. Proposed 'auto-zero' feedback TIA (trans-impedance amplifier) with interference rejection filter, where IRF is the interference rejection filter, LPF is the low pass filter

filter is used to provide additional gain, which also acts as an equalizer. Furthermore, it rejects the disturbances due to internal switching of the LED driver. In section 4, it has been mentioned that the internal switching frequency (f_{SW}) of the LED driver is taken as 500 kHz to ensure accurate current regulation [23]. Moreover, the data has been simultaneously transmitted using external switching circuit at 30 kHz. Both these frequencies have some obvious effects at the receiver. However, rejection of unwanted high frequency is required for faithful reception of the data pulse. This is achieved by the appropriate design of low-frequency Butterworth filter. In order to obtain additional gain and high-frequency noise rejection, the cut-off frequency of this low pass filter is set at 39.7 kHz with voltage gain of about

$$20\ dB \cdot \left[20 \log_{10}\left(1+\frac{R6}{R7}\right)\right].$$

Experimental results show a close match between the transmitted and received waveforms at a frequency of 30 kHz. As the frequency of external switching increases, the received waveform gradually deviates from the shape of the transmitted pulse. The calculated values of all components of the receiving section are shown in Table 2.

The third and final stage of the developed optical receiver is the data recovery unit, which consists of a sampler followed by a decision algorithm that will make the decision regarding the amplitude of sampled data. This is designed using *Arduino* microcontroller supported by *MATLAB*. The output of the low pass filter (V_{Out}) is sent to the analogue input pin of *Arduino* Mega 2560 interfaced with *MATLAB Simulink* to run the decision algorithm. Signal sent to the *Simulink* through *Arduino* is sampled and compared with a threshold value. The "Interval closed on right" and "Interval closed on left" checkboxes include the "Upper limit" and "Lower limit" within the working interval. The working *Simulink* model is shown in Fig. **7.** If the input lies within the range specified by the "Upper limit" and "Lower limit", the output is "TRUE" i.e. '1'. Whereas it is "FALSE" i.e. '0' if the input is outside the defined limit. For commercial use, where performance evaluation in terms of BER is not required, this block can be replaced by DSP processor.

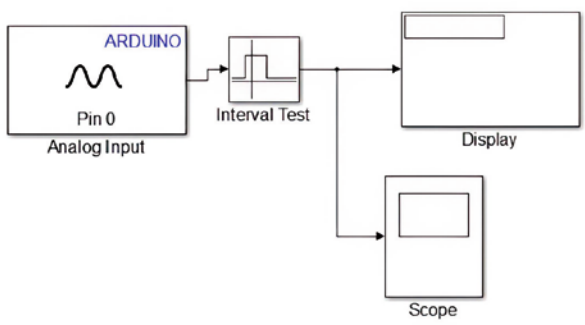

Fig. 7. *MATLAB Simulink* model for data recovery through *Arduino Mega*

6. ILLUMINATION PERFORMANCE

As mentioned in section 2, lighting simulation of the entire office space is done using the DIALux. Contribution of the ambient illuminance (E_{AL}) and illuminance of optical transmitter (E_{AP}) at each cubicle are separately figured out. It has been observed that the optical transmitter makes the main contribution of lighting to a given area, and this contribution is limited within the cabin, which provides zero CCI. The common space/corridor is illuminated by the five equally spaced CFLs, which also create ambient light interference. The simulated result reveals that the sole contribution from each access

Table 2. Component Details of Designed Optical Receiver

Component	Value	Component	Value
Photodiode (PD)	VISHAY TEMD7000X01	Capacitor (C1)	100 pF
Resistor (R1)	2 kohm	Capacitor (C2)	10 pF
Resistor (R2)	2 kohm	Capacitor (C3)	1000 pF
Resistor (R3)	20 kohm	Capacitor (C4)	10 nF
Resistor (R4)	20 kohm	Capacitor (C5)	0.01μF
Resistor (R5)	200 kohm	Capacitor (C6)	14 nF
Resistor (R6)	400 ohm	Capacitor (C7)	10 nF
Resistor (R7)	47 ohm	Opt. Amp (A1)	LTC6244
Resistor (R8)	1 kohm	Opt. Amp (A2)	LTC6244
Resistor (R9)	10 kohm	Opt. Amp (A3)	LP2904
Resistor (R10)	7.9 kohm	Opt. Amp (A4)	LM7171

point in their respective working areas is almost similar. This is understandable for the group of cubicles with identical room geometry. In order to verify the simulated result and most importantly to investigate the communication performance, practical experimentation is carried out considering a single cubicle.

To measure the contribution of an optical transmitter the complete working area is first divided into arrays of (5×5) grid points for grid specific data collection purposes. It is shown in Fig. 8.

A luxmeter is placed at each grid point and corresponding illuminance value is recorded. The average illuminance is the arithmetic mean of the illuminance values, measured at each grid point. The surface plot of illuminance distribution due to the optical transmitter is given in Fig. 9.

7. COMMUNICATION PERFORMANCE

To evaluate communication performances of the proposed system, the LED luminaire is mounted at a height of 1 m above the working area. The intensity of the optical source is modulated using an incoming binary data stream. The data enabled LED driver does this on-off keying modulation. Two types of testing are performed to assess the effectiveness of communication. In case of static evaluation scheme, a random 7-bit digital data is generated using shift register "Ex-Or" gate as shown in Fig. 10.

This sequence is connected to the data input of our proposed LED driver. Now the intensity-modulated data is received by the photodiode in the presence of daylight. Then the transmitted and received bit sequence is compared using an oscilloscope. Here, clock frequency for the transmitter and receiver section is kept (30 kHz) the same. The results, which are given in Section 8, show proper reception of transmitted random data even in the presence of daylight noise.

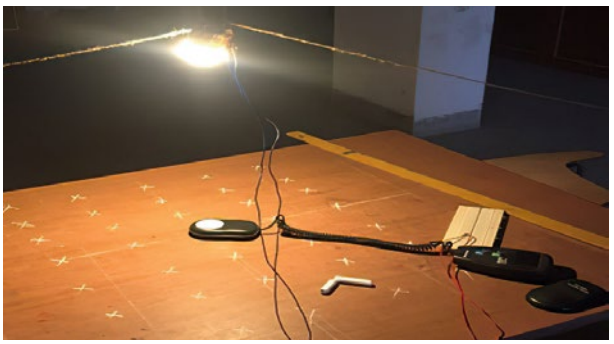

Fig. 8. Illuminance measurement on horizontal working surface

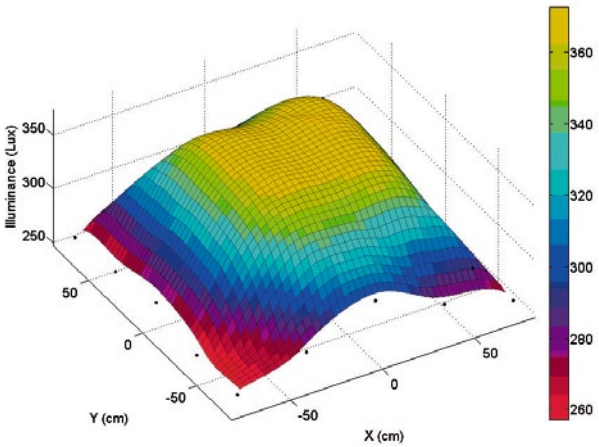

Fig. 9. Surface plot of illuminance distribution over the working area

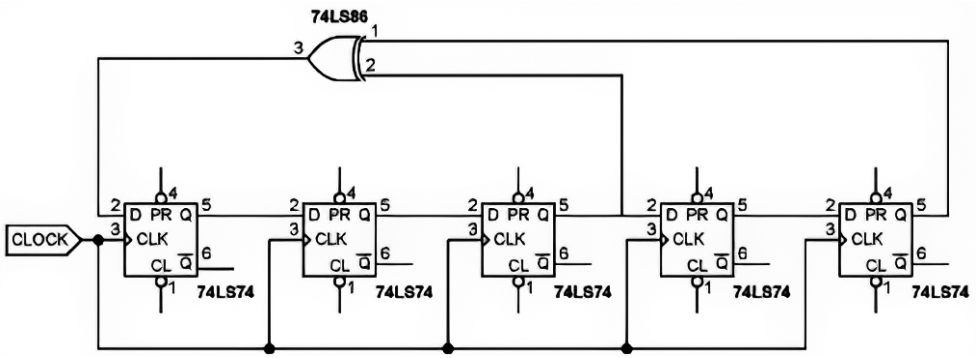

Fig. 10. Random sequence generator circuit

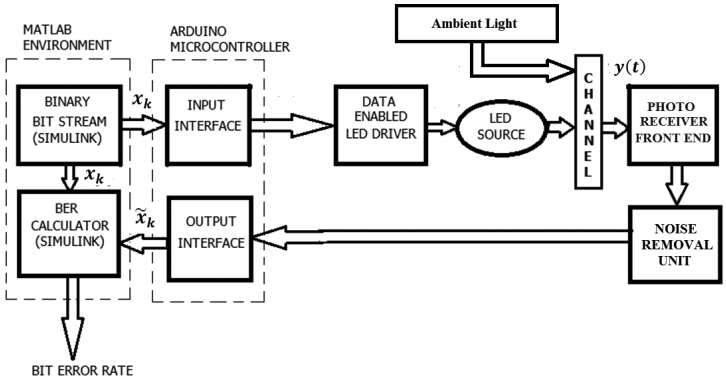

Fig. 11. Operation flow diagram of bit error rate measurement

To evaluate the proposed system in real time, it is necessary to transmit a continuous long stream of binary data and simultaneously receive them using an optical receiver in the presence of ambient light interference. The full procedure for real-time experimentation and performance evaluation based on the measurement of the bit error rate (BER) is described by the diagram presented in Fig. 11. Using DIALux simulations, it was found that a maximum 109 lx of ambient light creates interference and affects communication functionalities. For experimental testing of the proposed receiver's resistance to ambient light, a compact fluorescent lamp (CFL) that generates ambient light interference is used separately. In presence of this ambient light noise, BER is measured with the help of *Arduino* interfaced *MATLAB Simulink* environment.

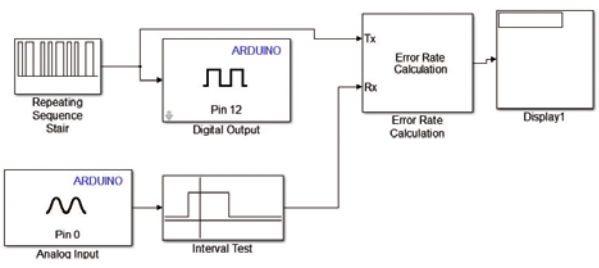

Fig. 12. *MATLAB Simulink* model for BER measurement through *Arduino Mega*

Here the role of *MATLAB Simulink* environment is two-fold. First, it generates a long test bit-stream *x (n),* which acts as input data for the designed LED driver and also at the time of receiving it performs BER calculation. The repeating sequence stair block of *Simulink* model is interfaced with the LED driver through *Arduino* microcontroller (ATmega 2560). The 'Digital Output' pin of the *Arduino* is connected to the data input of the LED driver. Then the transmitted signal is received by the photo detector, which is placed on an illuminated working surface. The output signal of the first two blocks of the optical source, described in section 5, is fed to the output of the ATmega 2560 analogue input, which acts as the output device of the system. The *MATLAB Simulink* model compares the transmitted bit sequence *x (n)* and received bit pattern $\overline{x}(n)$ and gives the bit error rate of the system. The *Simulink* model for data generation and reception is shown in Fig. 12.

8. RESULTS AND DISCUSSION

Preliminary experimentation was conducted with the developed system to judge the waveform retrieval capability of the data recovery unit. A square pulse of 30 kHz was transmitted by modulating the LED source. Figs.13(a) and 13(b) represents the

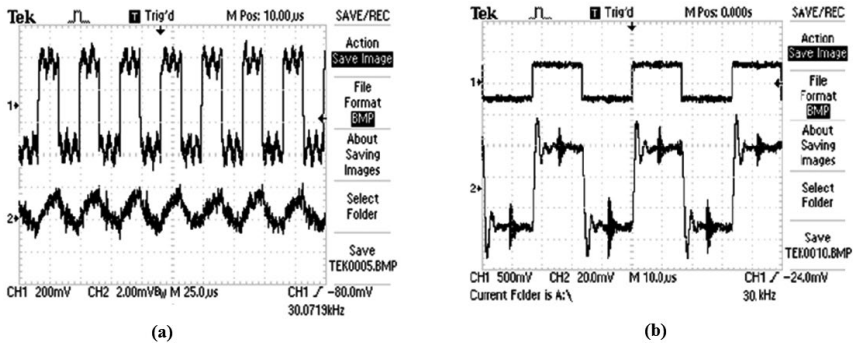

Fig. 13. Measured transmitted and received waveform pattern at 30 kHz without TIA (a) and with TIA (b)

measured waveforms of transmitted and received signals without TIA and with TIA. These two sets of waveforms indicate the importance of trans-impedance amplifier unit as mentioned in Section 5.

If we consider zero noise and zero inter-symbol interference (ISI) then the decision-circuit output signal voltage, $v_{out}(t)$, should always exceed the threshold voltage when a 1 is sent and should be less than the threshold when 0 is sent. However, from the practical point of view of communication, as in the proposed system, there are deviations from the average value of $v_{out}(t)$ caused by various noises, interference from neighbouring pulses, etc.. The threshold voltage, V_{th}, for performing the interval test, as shown in Fig. 12 is assumed as 50 mV, which is half of the minimum peak to peak measured voltage at grid points.

Theoretically, the Gaussian approximation is used to calculate the frequency of bit errors in the receiver. The following empirical relations given in equations (10) and (11) provide a measure of BER [25].

$$\text{BER} = P_e(Q) = \frac{1}{\sqrt{\pi}} \int_{Q/\sqrt{2}}^{\infty} e^{-x^2}\, dx = \frac{1}{2}\left[1 - erf\left(\frac{Q}{\sqrt{2}}\right)\right], \tag{10}$$

$$Q = \frac{v_{th} - b_{off}}{\sigma_{off}} = \frac{b_{on} - v_{th}}{\sigma_{on}} = \frac{b_{on} - b_{off}}{\sigma_{on} + \sigma_{off}}. \tag{11}$$

As discussed in Section 7, static and real-time evaluation of the communication performance of the proposed system is done for the real channel. Fig. 14 shows the transmitted and received bit sequence for a 7-bit random test data. From the figure, it is evident that 'auto-zero' feedback TIA successfully nullifies the external bias provided by the daylight and retrieves the transmitted data.

In the case of real-time validation, as presented in Fig. 11, practically obtained bit error rate is in the order of 10^{-8} in the presence of ambient daylight. However, the bit error rate is augmented with increment in signal to interference plus noise ratio (SINR). The interference rejection filter at the receiver section eliminates most of the harmonics generated by the ambient light sources. However, some high-frequency analogues can act as an unavoidable internal noise of the system. Deviations of BER and SINR with increase in ambient illuminance are shown in Fig. 15.

Measured illuminance distribution shows an average light level of 231.9 lx over the working area inside one cubicle. Considering this single contribution of the optical transmitter and ambient light, DIALux simulation is done for entire office space. Five CFLs, primarily installed to illuminate the common corridor, also contribute to the working area inside all cubicles. The result (given in Table 3) shows satisfactory lighting performance over all the working areas and corridor in terms of horizontal illuminance and overall illuminance uniformity. Due to the symmetrical nature of the room and luminaries arrangement, almost identical illuminance distribution was obtained in all opposite-standing cabins. The isolux curves at the working area (in cubicle C3) and common corridor are shown in Fig. 16.

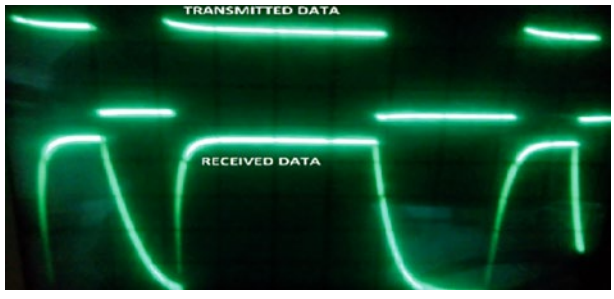

Fig. 14. Measured transmitted and received bit pattern (in presence of daylight)

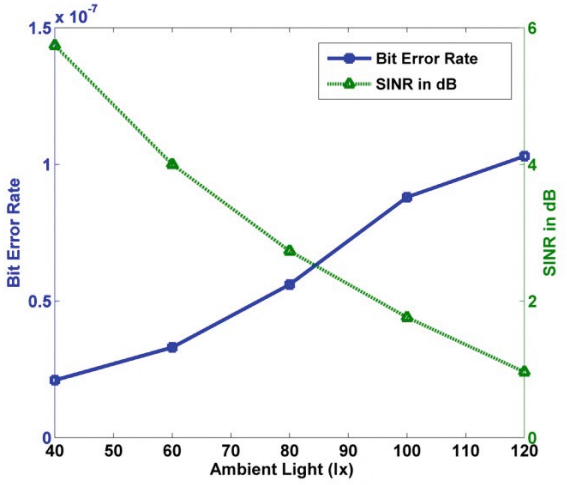

Fig. 15. Variation of BER and SINR in different ambient light intensity

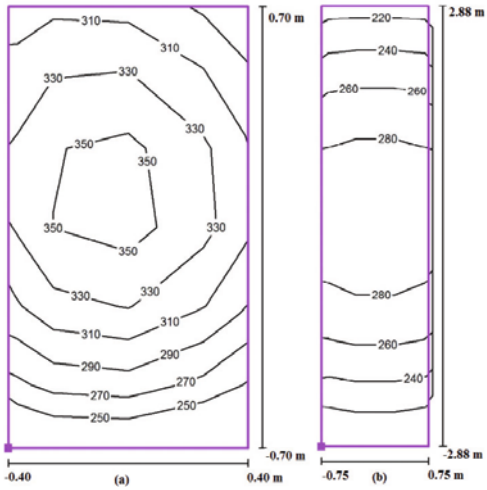

Fig. 16. Isolux curves at working area inside cubicle (a) and in common corridor (b)

From the simulated results, it was observed that the contribution by the ambient light source over the working area inside the cubicle varies between 41 lx and 109 lx. As ambient light increases over the work area, SINR gradually decreases from 5.94 dB to 0.96 dB. However, the experimental result shows satisfactory BER in the order of 10^{-7} within this interval. From the results obtained, we can conclude that our system demonstrates the best communication characteristics in terms of BER and data transfer speed in relation to the mentioned article [14].

9. CONCLUSION

The data transmission in optical wireless communication (OWC) with incoherent light sources is realized through intensity modulation and direct detection (IM/DD) using multi-level pulse amplitude modulation (*2*-PAM). For this purpose, a low-cost data-enabled LED driver along with its receiver counterpart is proposed. The primary aim of this work is to bridge the gap between lighting and communication, which is established through an application-based study. This study proposes a promising VLC supportive lighting solution applicable to an office environment. In addition to transmitting data, all access points (APs) contribute to lighting working areas, while light sources intended solely for lighting, create interference. The receiver section of the proposed system restricts the BER in the range of 10^{-7} even in the presence of ambient interferences. Moreover, the average horizontal illuminance and illuminance uniformity over all the working areas go with the CIE/ISO recommendation.

Table 3. Lighting Performance over Different Working Area

Working area	Average horizontal illuminance (lx)	Overall illuminance uniformity
Left lower (C1)	311	0.73
Left middle (C2)	338	0.76
Left upper (C3)	314	0.74
Right lower (C4)	311	0.73
Right middle (C5)	338	0.76
Right upper (C6)	314	0.74
Common corridor	260	0.77

REFERENCES

1. Narendran N., Gu Y. Life of LED-based white light sources. Journal of display technology, 2005. #1(1), 167 p.

2. Kocaman B., Rüstemli S. Comparison of LED and HPS luminaires in terms of energy savings at tunnel illumination. Light & Engineering, 2019. V27, #1, pp. 67–74.

3. Amelkina S.A., Zheleznikova O.E., Sinitsyna L.V. On the efficiency of lighting by LEDs in visual work. Light & Engineering, 2018. V26, #3, pp. 81–87.

4. Green R. J., Joshi H., Higgins M.D., Leeson M.S. Recent developments in indoor optical wireless systems. IET communications, 2008. V2, #1, pp. 3–10.

5. Gancarz J., Elgala H., Little TD. Impact of lighting requirements on VLC systems. IEEE Communications Magazine, 2013. V19, #51(12), pp. 34–41.

6. Chatterjee S., Sabui D. Daylight integrated indoor VLC architecture: An energy-efficient solution. Trans Emerging Tel Tech. 2019, e3800.

7. Markov M., Grigoriev Y.G. WI-FI technology–an uncontrolled global experiment on the health of man-

kind. Electromagnetic biology and medicine, 2013. V32, #2, pp. 200–208.

8. Miyahara S., Aono S., Matsumoto Y. Preproduction of LED driver for visible light communications and evaluation of response performance of visible LED. Technical report of IEICE, ICD2005–44, 2005. pp. 25–30.

9. O'Brien D. C., Faulkner G., Le Minh H., Bouchet O., El Tabach M., Wolf M., Langer K.D. Home access networks using optical wireless transmission. In 2008 IEEE19th International Symposium on Personal, Indoor and Mobile Radio Communications, IEEE, 2008, pp. 1–5.

10. Vučić J., Kottke C., Nerreter S., Langer K.D., Walewski J.W. 513 Mbit/s visible light communications link based on DMT-modulation of a white LED. Journal of lightwave technology, 2010. V28, #24, pp. 3512–3518.

11. McKendry J.J., Massoubre D., Zhang S., Rae B.R., Green R.P., Gu E., Dawson M.D. Visible-light communications using a CMOS-controlled micro-light-emitting-diode array. Journal of lightwave technology, 2011.V30, #1, pp. 61–67.

12. Elgala H., Mesleh R., Haas H. Indoor optical wireless communication: potential and state-of-the-art. IEEE Communications Magazine, 2011. V49, #9, pp. 56–62.

13. Sindhubala K., Vijayalakshmi B. Survey on noise sources and restrain techniques in visible-light communication. Light & Engineering, 2016. V24, #2, pp. 107–117.

14. Sindhubala K., Vijayalakshmi B. Design and implementation of optical receiver for visible light communication to reduce ambient light noise. Light & Engineering, 2017. V25, #2, pp. 139–146.

15. Din I., Kim H. Energy-efficient optical power control for data rate and illuminance provision in visible light communication. Light & Engineering, 2016. V24, #2, pp. 89–95.

16. Ho S. W., Duan J., Chen, C.S. Location-based information transmission systems using visible light communications. Transactions on Emerging Telecommunications Technologies, 2017. V28, #1, e2922.

17. ISO-8995–1:2002 (CIE-S008/E:2001) Lighting of work places – Part 1: Indoor

18. Kahn J. M., Barry J.R. Wireless infrared communications. Proceedings of the IEEE, 1997. V85, #2, pp. 265–298.

19. Chen Y., Sung C.W., Ho S.W., Wong W.S. BER analysis and power control for interfering visible light communication systems. Optik, 2017. V151, pp. 98–109.

20. Afgani M. Z., Haas H., Elgala H., Knipp D. Visible light communication using OFDM. In 2nd International Conference on Testbeds and Research Infrastructures for the Development of Networks and Communities, TRIDENTCOM, IEEE, 2006. 6 p.

21. Gfeller F. R., Bapst U. Wireless in-house data communication via diffuse infrared radiation. Proceedings of the IEEE, 1979. V67, #11, pp. 1474–1486.

22. Komine T., Nakagawa M. Fundamental analysis for visible-light communication system using LED lights. IEEE transactions on Consumer Electronics, 2004. V50, #1, pp. 100–107.

23. Texas Instruments, "60-W Common Anode-Capable Constant Current Buck LED Driver", LM3414, LM-3414HV datasheet, June 2010 [Revised November 2015].

24. Moreira A.J., Valadas R.T., de Oliveira Duarte A.M. Optical interference produced by artificial light. Wireless Networks, 1997. V3, #2, pp. 131–40.

25. Keiser G. Optical fiber communications. Wiley Encyclopedia of Telecommunications, 2003. Apr. 15.

Sourish Chatterjee
is pursuing his research study in the area of VLC at the Electrical Engineering Department of Jadavpur University. He completed the graduation course in Electronics and Communication Engineering from The Institution of Engineers (India) in 2008 followed by post-graduation course in Illumination Engineering from the Electrical Engineering Department of Jadavpur University in 2011. He has about eight years of teaching experience in the field of Electronics and Communication engineering. He is a Member of the IEI – The Institution of Engineers (India)

Biswanath Roy
is associated with the Electrical Engineering Department of Jadavpur University since 2000 at a faculty of Illumination Engineering. He completed Ph.D. (Engg.) in the field of Daylighting science in 1999 from the Jadavpur University after having M. Sc. (Tech.) in Optics & Optoelectronics from the Department of Applied Physics in 1993 and B. Sc. (Hons.) in Physics in 1989, both from the University of Calcutta. He is a Life Fellow of Indian Society of Lighting Engineers (ISLE), a Life Member of the IEI – The Institution of Engineers (India)